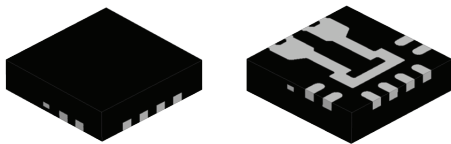


High Sensitivity, 1 MHz, GMR-Based Current Sensor IC in Space-Saving Low Resistance QFN package

FEATURES AND BENEFITS

- High sensitivity current sensor IC for sensing up to 5 A (DC or AC)
- 1 MHz bandwidth with response time <math><550\text{ ns}</math>
- Low noise: 6 mA(rms) at 1 MHz
- Analog output proportional to AC and DC current
- Single 3.3 V supply operation
- High DC PSRR enables use with low accuracy power supplies or batteries (3 to 4.5 V operation)
- 1.1 m Ω primary conductor resistance results in low power loss
- Small surface mount QFN package for space-constrained applications

PACKAGE



12-contact QFN
3 mm \times 3 mm \times 0.75 mm
(ES package)

Not to scale

DESCRIPTION

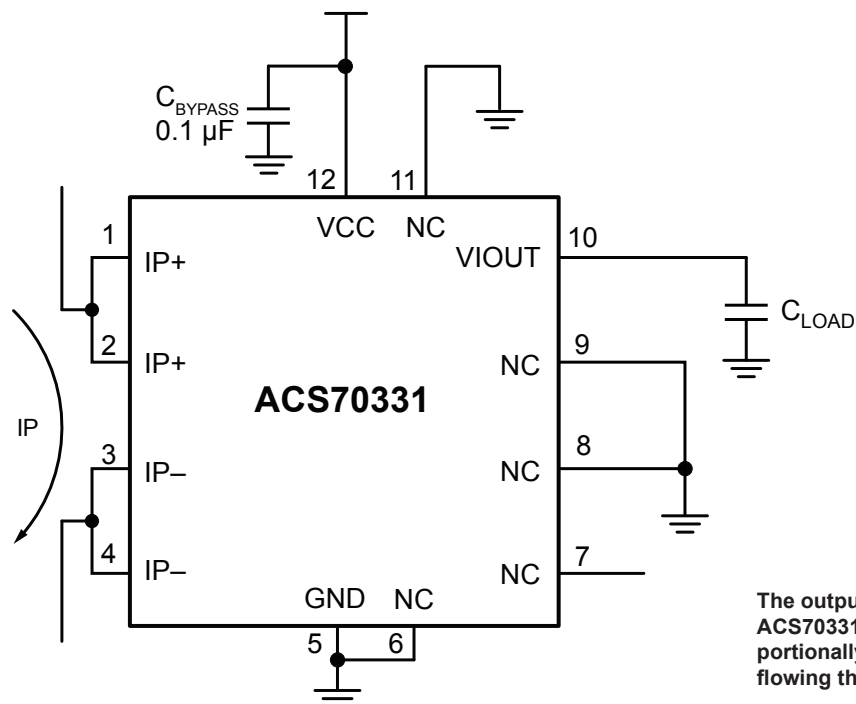
The ACS70331 is Allegro's first integrated, high sensitivity, current sensor IC for <math><5\text{ A}</math> current sensing applications. It incorporates giant magneto-resistive (GMR) technology that is 25 times more sensitive than traditional Hall-effect sensors to sense the magnetic field generated by the current flowing through the low resistance, integrated primary conductor.

The analog output provides a low noise high-speed signal, which is proportional to the current flowing through the primary. The response time of the part is typically 535 ns. The ACS70331 is offered in four factory-programmed sensitivity and offset levels to optimize performance over the desired current measurement range.

The differential configuration of the GMR elements, relative to the integrated current conductor, provides significant rejection of stray magnetic fields, resulting in stable operation even in magnetically noisy environments.

The ACS70331 operates from a single 3.3 V power supply and is qualified over the full commercial temperature range of -40°C to 85°C . It is offered in a low-profile space-saving surface mount QFN package.

TYPICAL APPLICATION



The output, VIOOUT, of the ACS70331 responds proportionally to the current flowing through IP.

SELECTION GUIDE

| Part Number | Current Sensing Range, I_{PR} (A) | Sens (Typ) (mV/A) | T_A (°C) | Package | Packing [1] |
|--------------------|-------------------------------------|-------------------|------------|--|----------------------|
| ACS70331EESA-2P5U3 | 0 to 2.5 | 800 | -40 to 85 | 12-contact QFN with fused current loop | 1500 pieces per reel |
| ACS70331EESA-2P5B3 | ±2.5 | 400 | | | |
| ACS70331EESA-005U3 | 0 to 5 | 400 | | | |
| ACS70331EESA-005B3 | ±5 | 200 | | | |

[1] Contact Allegro for additional packing options.

ABSOLUTE MAXIMUM RATINGS

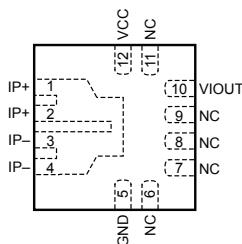
| Characteristic | Symbol | Notes | Rating | Units |
|---------------------------------------|-------------------|--|------------|-------|
| Supply Voltage | V_{CC} | | 7 | V |
| Reverse Supply Voltage | V_{RCC} | | -0.1 | V |
| Output Voltage | V_{IOUT} | | 6 | V |
| Reverse Output Voltage | V_{RIOUT} | | -0.1 | V |
| Working Voltage | $V_{WORKING}$ | Voltage applied between pins 1 to 4 and pins 5 to 12 | 100 | V |
| Maximum Continuous Current [2] | $I_P(max)$ | | ±10 | A |
| Maximum Continuous External Field [3] | B | | ±50 | G |
| Nominal Operating Ambient Temperature | T_A | Range E | -40 to 85 | °C |
| Maximum Junction Temperature [2] | $T_J(max)$ | | 100 | °C |
| Maximum Soldering Temperature [4] | $T_{solder}(max)$ | | 265 | °C |
| Storage Temperature | T_{stg} | | -65 to 125 | °C |

[2] Continuous currents above this may result in changes in performance. See lifetime drift section for sensor drift under different temperature and current conditions. Also, see Thermal Performance and Overcurrent Capability section for allowable constant and transient currents.

[3] Continuous magnetic fields above this may result in changes in performance.

[4] The ACS70331 should be soldered using Allegro's recommended soldering profile in (<http://www.allegromicro.com/en/Design-Center/Technical-Documents/Semiconductor-Packaging-Publications/Soldering-Methods-for-Allegro-Products.aspx>). Standard soldering tips will over-stress the device, resulting in shifts in performance. For rework, it is recommended to use hot plates and heat guns/pencils, keeping the temperature of the device below the Maximum Soldering Temperature.

PINOUT DIAGRAM AND TERMINAL LIST TABLE

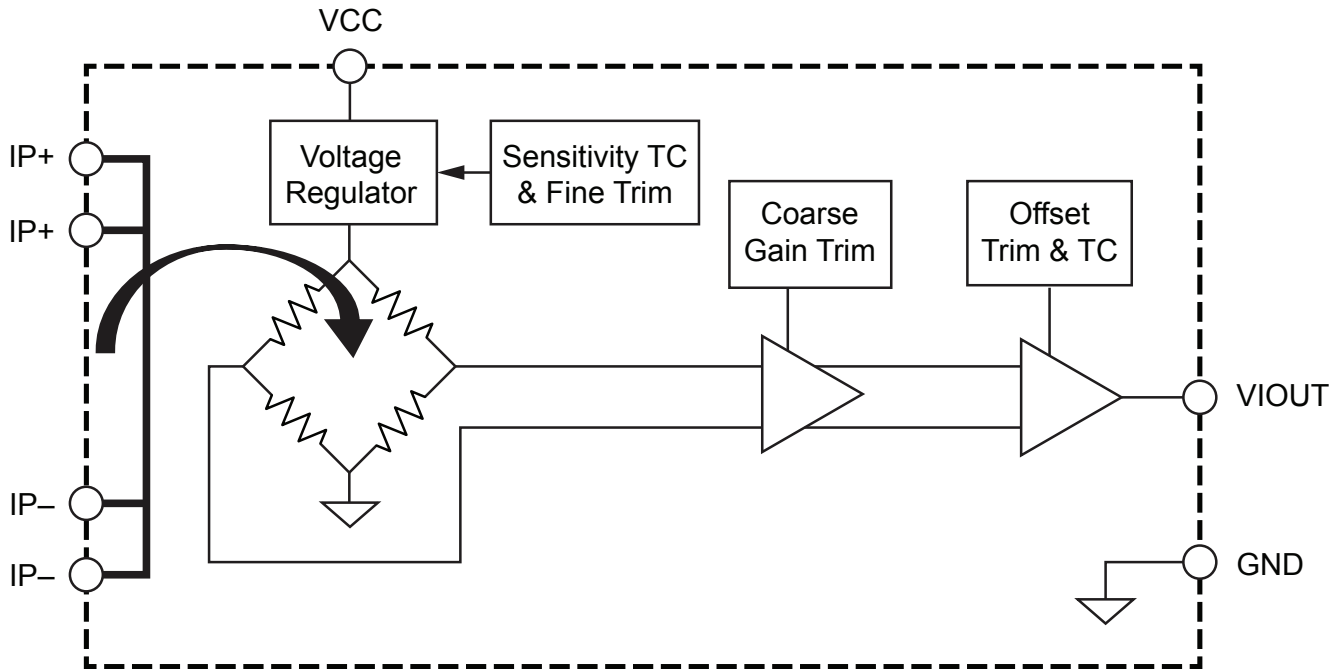


Package ES, 12-Pin QFN
Pinout Diagram

Terminal List Table

| Number | Name | Description |
|-------------|-------|---|
| 1, 2 | IP+ | Terminals for current being sensed; fused internally |
| 3, 4 | IP- | Terminals for current being sensed; fused internally |
| 5 | GND | Device ground terminal |
| 6, 8, 9, 11 | NC | No connection, ground for the best ESD performance |
| 7 | NC | This pin should be left unconnected during normal operation |
| 10 | VIOUT | Analog output representing the current flowing through IP |
| 12 | VCC | Device power supply terminal |

FUNCTIONAL BLOCK DIAGRAM



COMMON ELECTRICAL CHARACTERISTICS [1]: Valid over full range of T_A , and $V_{CC} = 3.3$ V, unless otherwise specified

| Characteristic | Symbol | Test Conditions | Min. | Typ. | Max. | Unit |
|-----------------------------------|---------------------|---|------|-----------------|---------|--|
| ELECTRICAL CHARACTERISTICS | | | | | | |
| Supply Voltage | V_{CC} | | 3.0 | 3.3 | 4.5 | V |
| Supply Current | I_{CC} | $V_{CC}(\min) \leq V_{CC} \leq V_{CC}(\max)$, no load on VIOUT, fuses powered down | – | 4.5 | 6 | mA |
| | $I_{CC_START_UP}$ | $V_{CC}(\min) \leq V_{CC} \leq V_{CC}(\max)$, no load on VIOUT, fuses powered (from time when V_{CC} rises above $V_{CC}(\min)$ to t_{FPD}) | – | – | 7.5 | mA |
| Primary Conductor Resistance | R_{IP} | $T_A = 25^\circ\text{C}$ | – | 1.1 | – | m Ω |
| Primary Conductor Inductance | L_{IP} | Measured at 1 MHz | – | 1.7 | – | nH |
| Power On Time | t_{PO} | $T_A = 25^\circ\text{C}$ | – | 5 | – | μs |
| Fuse Power Down Time [2] | t_{FPD} | $T_A = 25^\circ\text{C}$ | – | 80 | 120 [3] | μs |
| OUTPUT CHARACTERISTICS | | | | | | |
| Output Resistive Load | R_L | VIOUT to GND or VIOUT to VCC | 22 | – | – | k Ω |
| Output Capacitive Load | C_L | VIOUT to GND, output is stable, slew rate and bandwidth are reduced | – | – | 100 | pF |
| | | VIOUT to GND, maintains BW | – | – | 50 | pF |
| Source Current | I_{SOURCE} | $T_A = 25^\circ\text{C}$ | – | 0.4 | – | mA |
| Sink Current | I_{SINK} | $T_A = 25^\circ\text{C}$ | – | 0.5 | – | mA |
| Saturation Voltage [4] | V_{SAT_HIGH} | $V_{CC}(\min) < V_{CC} < V_{CC}(\max)$; $R_L = 22$ k Ω to GND | 2.8 | $V_{CC} - 0.15$ | – | V |
| | V_{SAT_LOW} | $V_{CC}(\min) < V_{CC} < V_{CC}(\max)$; $R_L = 22$ k Ω to VIOUT | – | 20 | 200 | mV |
| Bandwidth | BW | –3 dB bandwidth | – | 1 | – | MHz |
| Response Time | $t_{RESPONSE}$ | 1 V swing on VIOUT, 80% to 80% | – | 535 | – | ns |
| Rise Time | t_r | 1 V swing on VIOUT, 10% to 90% | – | 460 | – | ns |
| Propagation Delay | t_{pd} | 1 V swing on VIOUT, 20% to 20% | – | 220 | – | ns |
| Noise Density | I_{ND} | Input referred noise density | – | 6 | – | $\mu\text{A}_{RMS}/\sqrt{(\text{Hz})}$ |
| Noise | I_N | Input reference noise; $T_A = 25^\circ\text{C}$, Bandwidth = 1 MHz | – | 6 | – | mA_{RMS} |
| Hysteresis | I_H | $T_A = 25^\circ\text{C}$; change in the output at zero current after a ± 10 A pulse of current through the sensor | – | 10 | 20 | mA |
| | | $T_A = 25^\circ\text{C}$; change in the output at zero current after a ± 100 A pulse (~20 ms in duration) of current through the sensor | – | 20 | – | mA |

Continued on next page...

COMMON ELECTRICAL CHARACTERISTICS [1] (continued): Valid over full range of T_A , and $V_{CC} = 3.3$ V, unless otherwise specified

| Characteristic | Symbol | Test Conditions | Min. | Typ. | Max. | Unit |
|---|----------------------|--|------|------|------|------|
| Stray Field Sensitivity Error Ratio [5] | STER _{SENS} | Measured at 20 G, worst case field orientation | – | 0.2 | – | %/G |
| Stray Field Offset Error Ratio [5] | STER _{OFF} | Measured at 20 G, worst case field orientation | – | 3.8 | – | mA/G |
| Power Supply Rejection Ratio | PSRR | DC to 100 Hz, 100 mV pk-pk on VCC | – | 40 | – | dB |
| | | 100 Hz to 100 kHz, 100 mV pk-pk on VCC | – | 30 | – | dB |
| Power Supply Offset Error | $V_{OE(PS)}$ | Change in offset voltage over $3.0\text{ V} < V_{CC} < 4.5\text{ V}$ | – | ±10 | – | mV |
| Power Supply Sensitivity Error | $E_{SENS(PS)}$ | Change in sensitivity over $3.0\text{ V} < V_{CC} < 4.5\text{ V}$ | – | ±0.5 | – | % |
| Nonlinearity | E_{LIN} | | – | ±0.2 | – | % |

[1] Device may be operated at higher ambient, T_A , and internal leadframe temperatures, T_A , provided that the Maximum Junction Temperature, $T_J(\text{max})$, is not exceeded.

[2] The internal fuses (non-volatile memory used for factory programming) will be powered for t_{FPD} after V_{CC} goes above $V_{CC}(\text{min})$. After this time, the fuse states will have been saved to volatile memory, and the fuses will be powered down to save power. This means that for t_{FPD} after powering the device, I_{CC} will be around 1 mA higher than specified (I_{CC}).

[3] This limit is based on simulation and is not tested in production.

[4] See Ideal Output Transfer Curve section.

[5] See Current Sensing Method using GMR and Stray Field Immunity section.

ACS70331EESA-2P5U3 PERFORMANCE CHARACTERISTICS: Valid over full range of T_A , and $V_{CC} = 3.3$ V, unless otherwise specified

| Characteristic | Symbol | Test Conditions | Min. | Typ. [1] | Max. | Unit |
|--|---------------|---|------|-----------|------|------|
| NOMINAL PERFORMANCE [2] | | | | | | |
| Current Sensing Range | I_{PR} | | 0 | – | 2.5 | A |
| Sensitivity | Sens | $I_{PR(min)} < I_P < I_{PR(max)}$ | – | 800 | – | mV/A |
| Zero Current Output Voltage | $V_{IOUT(Q)}$ | $I_P = 0$ mA, $T_A = 25^\circ\text{C}$ | – | 0.25 | – | V |
| ACCURACY PERFORMANCE | | | | | | |
| Total Output Error [3] | E_{TOT} | Measured at $I_P = I_{PR(max)}$, $T_A = 25^\circ\text{C}$ | – | ± 2 | – | % |
| | | Measured at $I_P = I_{PR(max)}$, $T_A = -40^\circ\text{C}$ to 85°C | – | ± 5 | – | % |
| TOTAL OUTPUT ERROR COMPONENTS [4][5] $E_{TOT} = E_{SENS} + 100 \times V_{OE}/(\text{Sens} \times I_P)$ | | | | | | |
| Sensitivity Error | E_{sens} | Measured at $I_P = I_{PR(max)}$, $T_A = 25^\circ\text{C}$ | – | ± 1.5 | – | % |
| | | Measured at $I_P = I_{PR(max)}$, $T_A = -40^\circ\text{C}$ to 85°C | – | ± 3 | – | % |
| Offset Voltage | V_{OE} | $I_P = 0$ A, $T_A = 25^\circ\text{C}$ | – | ± 30 | – | mV |
| | | $I_P = 0$ A, $T_A = -40^\circ\text{C}$ to 85°C | – | ± 70 | – | mV |

[1] Typical values with +/- are 3 sigma values.

[2] See Ideal Output Transfer Curve section.

[3] Percentage of I_P , with $I_P = I_{PR(max)}$.

[4] A single part will not have both the maximum/minimum sensitivity error and maximum/minimum offset voltage, as that would violate the maximum/minimum total output error specification. Also, 3 sigma distribution values are combined by taking the square root of the sum of the squares. See Application Information section.

[5] See Lifetime Drift section for accuracy drift under different application temperatures, currents, and fields.

ACS70331EESA-2P5B3 PERFORMANCE CHARACTERISTICS: Valid over full range of T_A , and $V_{CC} = 3.3$ V, unless otherwise specified

| Characteristic | Symbol | Test Conditions | Min. | Typ. [1] | Max. | Unit |
|--|---------------|---|------|-----------|------|------|
| NOMINAL PERFORMANCE [2] | | | | | | |
| Current Sensing Range | I_{PR} | | -2.5 | – | 2.5 | A |
| Sensitivity | Sens | $I_{PR(min)} < I_P < I_{PR(max)}$ | – | 400 | – | mV/A |
| Zero Current Output Voltage | $V_{IOUT(Q)}$ | $I_P = 0$ mA, $T_A = 25^\circ\text{C}$ | – | 1.5 | – | V |
| ACCURACY PERFORMANCE | | | | | | |
| Total Output Error [3] | E_{TOT} | Measured at $I_P = I_{PR(max)}$, $T_A = 25^\circ\text{C}$ | – | ± 2 | – | % |
| | | Measured at $I_P = I_{PR(max)}$, $T_A = -40^\circ\text{C}$ to 85°C | – | ± 3 | – | % |
| TOTAL OUTPUT ERROR COMPONENTS [4][5] $E_{TOT} = E_{SENS} + 100 \times V_{OE}/(\text{Sens} \times I_P)$ | | | | | | |
| Sensitivity Error | E_{sens} | Measured at $I_P = I_{PR(max)}$, $T_A = 25^\circ\text{C}$ | – | ± 1.5 | – | % |
| | | Measured at $I_P = I_{PR(max)}$, $T_A = -40^\circ\text{C}$ to 85°C | – | ± 3 | – | % |
| Offset Voltage | V_{OE} | $I_P = 0$ A, $T_A = 25^\circ\text{C}$ | – | ± 15 | – | mV |
| | | $I_P = 0$ A, $T_A = -40^\circ\text{C}$ to 85°C | – | ± 45 | – | mV |

[1] Typical values with +/- are 3 sigma values.

[2] See Ideal Output Transfer Curve section.

[3] Percentage of I_P , with $I_P = I_{PR(max)}$.

[4] A single part will not have both the maximum/minimum sensitivity error and maximum/minimum offset voltage, as that would violate the maximum/minimum total output error specification. Also, 3 sigma distribution values are combined by taking the square root of the sum of the squares. See Application Information section.

[5] See Lifetime Drift section for accuracy drift under different application temperatures, currents, and fields.

ACS70331EESA-005U3 PERFORMANCE CHARACTERISTICS: Valid over full range of T_A , and $V_{CC} = 3.3$ V, unless otherwise specified

| Characteristic | Symbol | Test Conditions | Min. | Typ. [1] | Max. | Unit |
|--|---------------|---|------|-----------|------|------|
| NOMINAL PERFORMANCE [2] | | | | | | |
| Current Sensing Range | I_{PR} | | 0 | – | 5 | A |
| Sensitivity | Sens | $I_{PR(min)} < I_P < I_{PR(max)}$ | – | 400 | – | mV/A |
| Zero Current Output Voltage | $V_{IOUT(Q)}$ | $I_P = 0$ mA, $T_A = 25^\circ\text{C}$ | – | 0.25 | – | V |
| ACCURACY PERFORMANCE | | | | | | |
| Total Output Error [3] | E_{TOT} | Measured at $I_P = I_{PR(max)}$, $T_A = 25^\circ\text{C}$ | – | ± 2 | – | % |
| | | Measured at $I_P = I_{PR(max)}$, $T_A = -40^\circ\text{C}$ to 85°C | – | ± 3 | – | % |
| TOTAL OUTPUT ERROR COMPONENTS [4][5] $E_{TOT} = E_{SENS} + 100 \times V_{OE}/(\text{Sens} \times I_P)$ | | | | | | |
| Sensitivity Error | E_{sens} | Measured at $I_P = I_{PR(max)}$, $T_A = 25^\circ\text{C}$ | – | ± 1.5 | – | % |
| | | Measured at $I_P = I_{PR(max)}$, $T_A = -40^\circ\text{C}$ to 85°C | – | ± 3 | – | % |
| Offset Voltage | V_{OE} | $I_P = 0$ A, $T_A = 25^\circ\text{C}$ | – | ± 15 | – | mV |
| | | $I_P = 0$ A, $T_A = -40^\circ\text{C}$ to 85°C | – | ± 45 | – | mV |

[1] Typical values with +/- are 3 sigma values.

[2] See Ideal Output Transfer Curve section.

[3] Percentage of I_P , with $I_P = I_{PR(max)}$.

[4] A single part will not have both the maximum/minimum sensitivity error and maximum/minimum offset voltage, as that would violate the maximum/minimum total output error specification. Also, 3 sigma distribution values are combined by taking the square root of the sum of the squares. See Application Information section.

[5] See Lifetime Drift section for accuracy drift under different application temperatures, currents, and fields.

ACS70331EESA-005B3 PERFORMANCE CHARACTERISTICS: Valid over full range of T_A , and $V_{CC} = 3.3$ V, unless otherwise specified

| Characteristic | Symbol | Test Conditions | Min. | Typ. [1] | Max. | Unit |
|--|---------------|---|------|-----------|------|------|
| NOMINAL PERFORMANCE [2] | | | | | | |
| Current Sensing Range | I_{PR} | | –5 | – | 5 | A |
| Sensitivity | Sens | $I_{PR(min)} < I_P < I_{PR(max)}$ | – | 200 | – | mV/A |
| Zero Current Output Voltage | $V_{IOUT(Q)}$ | $I_P = 0$ mA, $T_A = 25^\circ\text{C}$ | – | 1.5 | – | V |
| ACCURACY PERFORMANCE | | | | | | |
| Total Output Error [3] | E_{TOT} | Measured at $I_P = I_{PR(max)}$, $T_A = 25^\circ\text{C}$ | – | ± 2 | – | % |
| | | Measured at $I_P = I_{PR(max)}$, $T_A = -40^\circ\text{C}$ to 85°C | – | ± 3 | – | % |
| TOTAL OUTPUT ERROR COMPONENTS [4][5] $E_{TOT} = E_{SENS} + 100 \times V_{OE}/(\text{Sens} \times I_P)$ | | | | | | |
| Sensitivity Error | E_{sens} | Measured at $I_P = I_{PR(max)}$, $T_A = 25^\circ\text{C}$ | – | ± 1.5 | – | % |
| | | Measured at $I_P = I_{PR(max)}$, $T_A = -40^\circ\text{C}$ to 85°C | – | ± 2.5 | – | % |
| Offset Voltage | V_{OE} | $I_P = 0$ A, $T_A = 25^\circ\text{C}$ | – | ± 15 | – | mV |
| | | $I_P = 0$ A, $T_A = -40^\circ\text{C}$ to 85°C | – | ± 45 | – | mV |

[1] Typical values with +/- are 3 sigma values.

[2] See Ideal Output Transfer Curve section.

[3] Percentage of I_P , with $I_P = I_{PR(max)}$.

[4] A single part will not have both the maximum/minimum sensitivity error and maximum/minimum offset voltage, as that would violate the maximum/minimum total output error specification. Also, 3 sigma distribution values are combined by taking the square root of the sum of the squares. See Application Information section.

[5] See Lifetime Drift section for accuracy drift under different application temperatures, currents, and fields.

THEORY OF OPERATION

GMR Sensing Elements

The ACS70331 uses GMR (giant magneto-resistive) elements to indirectly measure the current flowing through the package by measuring the field produced by the current. These elements operate differently than the Hall-effect sensors used in the majority of Allegro’s current sensors. The main advantage of GMR is that it is much more sensitive than the Hall-effect, making it ideal

for measuring small currents. This is what enables the ACS70331 to have over 25 times lower input-referred noise than Allegro’s lowest noise Hall-effect based current sensors. GMR elements are essentially resistors which change resistance with applied field. A typical representative response curve for the GMR elements used in the ACS70331 is shown in Figure 1. It is important to note that the applied field is parallel to the surface of the sensor instead of perpendicular to the sensor plane as with planar Hall sensors.

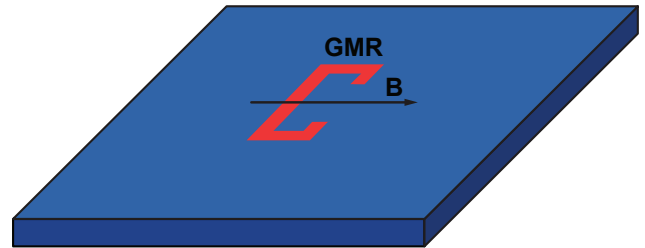
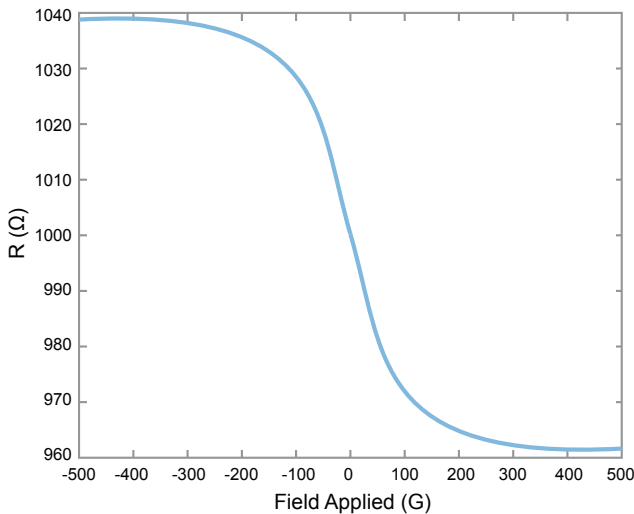


Figure 1: Typical Response Curve for GMR Elements

The equation describing this curve is:

$$R(B) = 1000 \left[1 - 0.04 \sin \left(\tan^{-1} \left(\frac{B}{100} \right) \right) \right]$$

This GMR element has a base resistance of around 1000 Ω that increases and decreases with field. It is important to note that a big difference between GMR and the Hall-effect is that GMR sensors saturate at relatively low fields, limiting the linear operating region. The linear region of the GMR elements used in the ACS70331 is around ±50 G.

Current Sensing Method using GMR and Stray Field Immunity

The internal construction of the ACS70331 is shown in Figure 2. The die sits above the primary current path such that magnetic field is produced in plane with the GMR elements on the die. GMR elements 1 and 2 sense field in the +X direction for positive IP current flow, and GMR elements 3 and 4 sense field in the -X direction for positive IP current flow. This enables differential measurement of the current and rejection of external stray fields.

The four GMR elements are arranged in a Wheatstone bridge configuration as shown in Figure 3 such that the output of the bridge is proportional to the differential field sensed by the four elements, rejecting common fields.

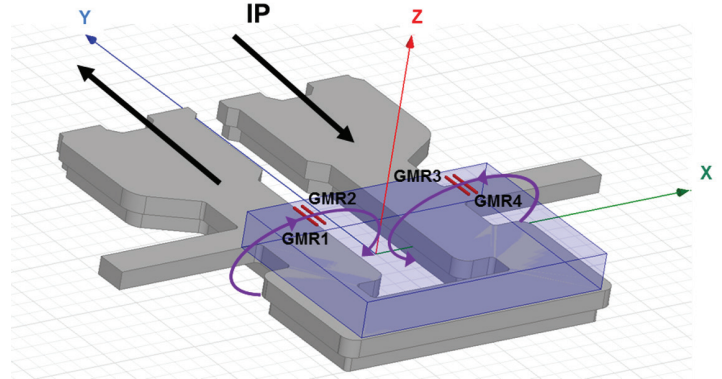


Figure 2: ACS70331 Internal Construction

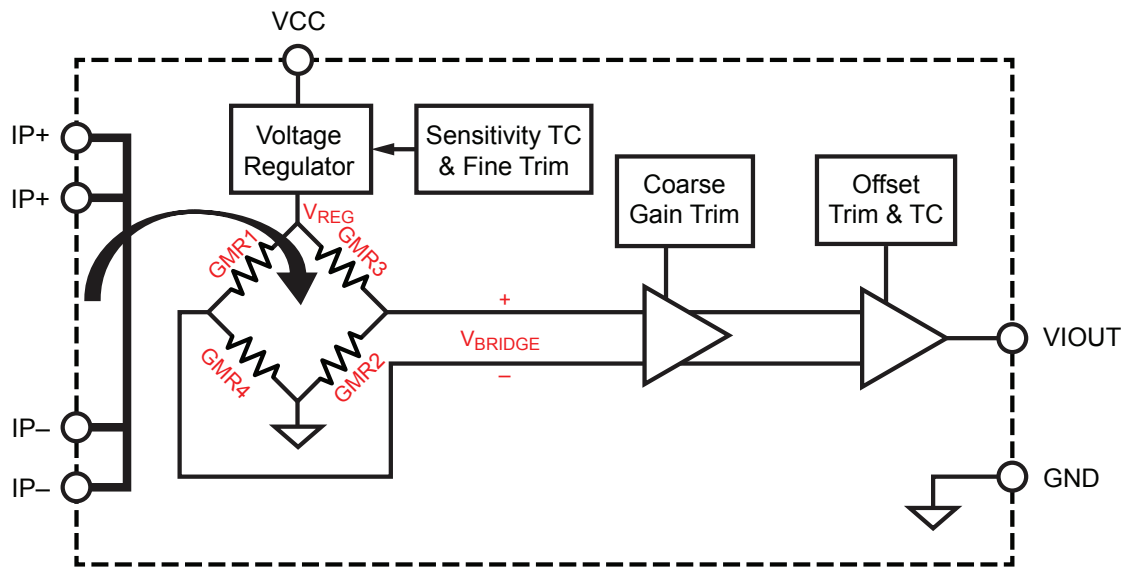


Figure 3: Wheatstone Bridge Configuration

The output of the bridge will be:

$$V_{BRIDGE} \propto V_{REG} \times I_P \times C_f$$

Here, C_f is the coupling factor from the primary current path to the GMR elements, which is around 4 G/A.

Theoretically, the bridge configuration will perfectly cancel out all external common-mode fields that could interfere with the sensor; however, the performance is limited by non-idealities, such as mismatch. Typical stray field rejection performance is given in Table 1 for stray fields of 20 G, which is much higher than what will be seen in most applications. Stray fields in the X direction result in

minimal sensitivity error but some offset error. Stray fields in the Y direction result in more sensitivity error and less offset error. Finally, stray fields in the Z direction result in essentially no error, as the GMR are not sensitive to fields in this dimension.

Table 1: Typical Stray Field Rejection Performance

| Field Level (G) | Field Orientation | Typical Sensitivity Error (%) | Typical Offset Error (mA) |
|-----------------|-------------------|-------------------------------|---------------------------|
| 20 | ±X | ±4.2 | ±76 |
| 20 | ±Y | ±3 | 15 |
| 20 | ±Z | 0 | 0 |

Gain and Offset Trim

The bridge configuration of the GMR elements in the ACS70331 make the gain and offset trim for the sensor relatively simple. As the bridge output voltage is proportional to the voltage driving it, that voltage is trimmed to compensate for all other nominal gain errors, as well as errors over temperature. Then, offset is trimmed out after the bridge voltage has been amplified. All trim codes are stored using fuses that are programmed at final test before locking the part.

Ideal Output Transfer Curve

The ideal output of the ACS70331 is:

$$V_{IOUT} = Sens \times I_P + V_{IOUT(Q)}$$

Different versions of the ACS70331 have different sensitivity (Sens) and zero current output voltage ($V_{IOUT(Q)}$) values in order to give different current measurement ranges. Unidirectional sensors start at 0.25 V with zero current through the primary and swing +2 V for full-scale current. Bidirectional sensors start at 1.5 V with zero current through the primary and swing ± 1 V for full-scale current. Figure 4 shows the ideal output transfer curves for each version of the ACS70331. The output curves show the typical saturation levels; however, the saturation could occur anywhere beyond the min/max saturation limits shown by the dashed lines. The stated accuracy of the sensor is only valid over the given current sensing range (I_{PR}).

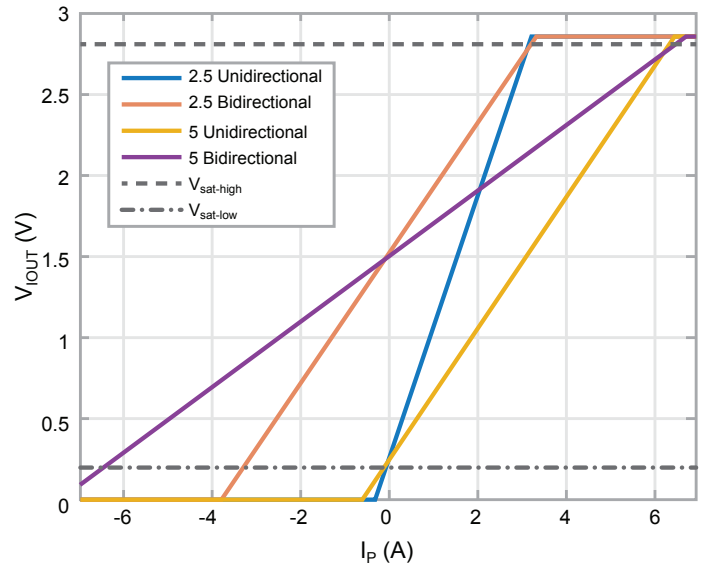


Figure 4: Ideal Output Transfer Curves

Power-On Behavior

The power-on behavior of the ACS70331 is shown in Figure 5. Once V_{CC} goes above $V_{CC(min)}$, it takes t_{PO} for the internal circuitry to fully power on and bring the output to the correct value. After t_{FPD} , the ACS70331 has saved the fuse values containing configuration and trim information to volatile registers and powered down the fuses to save power. During t_{FPD} , the ACS70331 uses the direct outputs from the fuses, meaning there is no change in configuration or trim when the fuses are powered down.

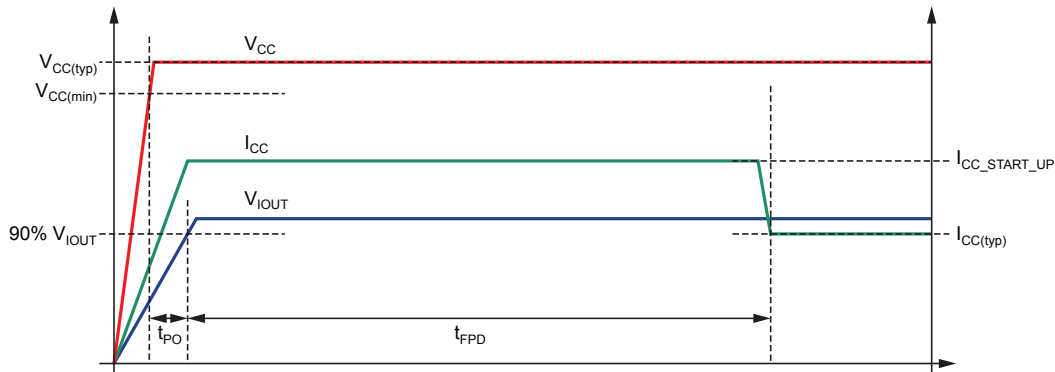
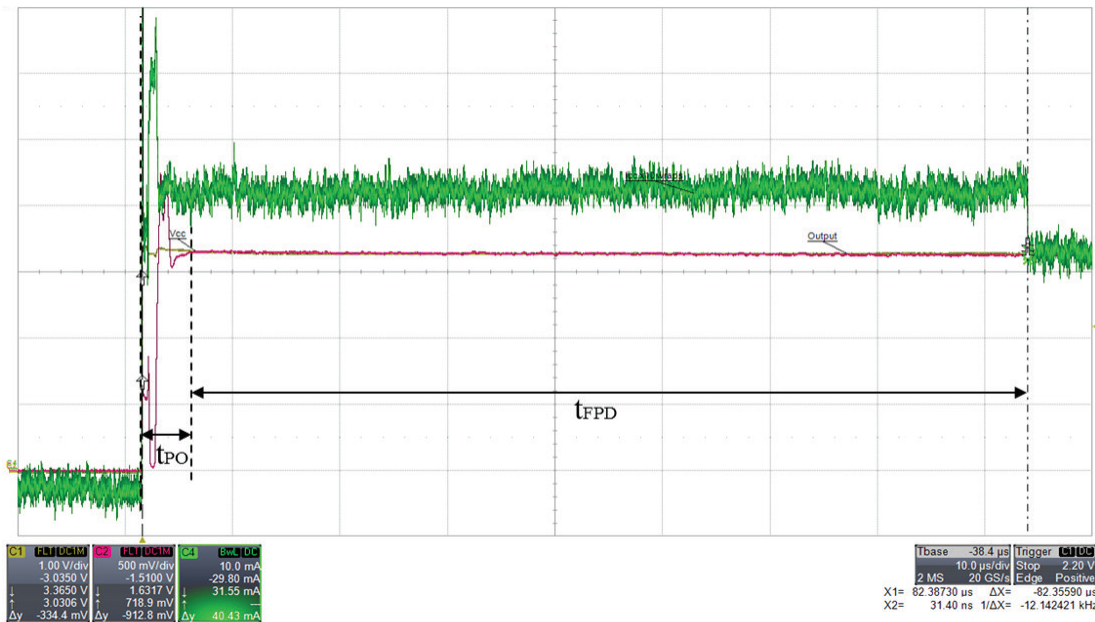


Figure 5: Power-On Behavior

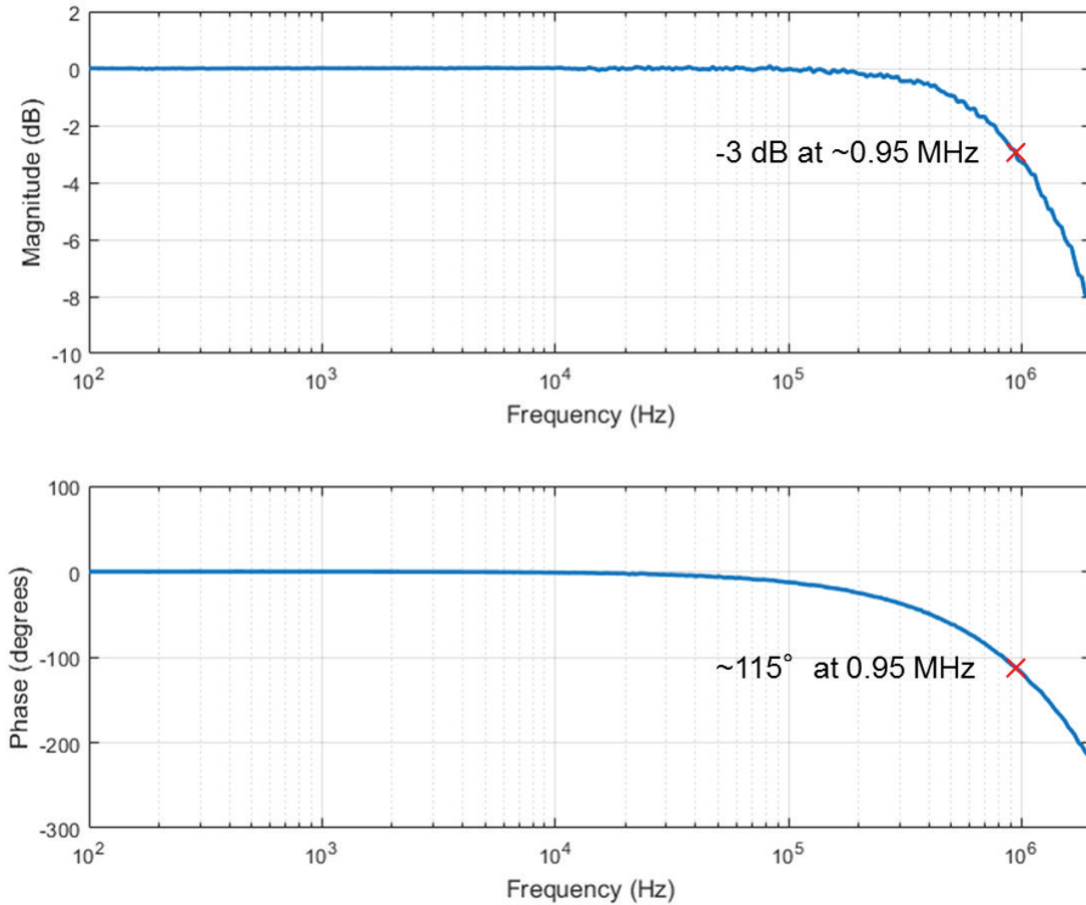


CHARACTERISTIC PERFORMANCE

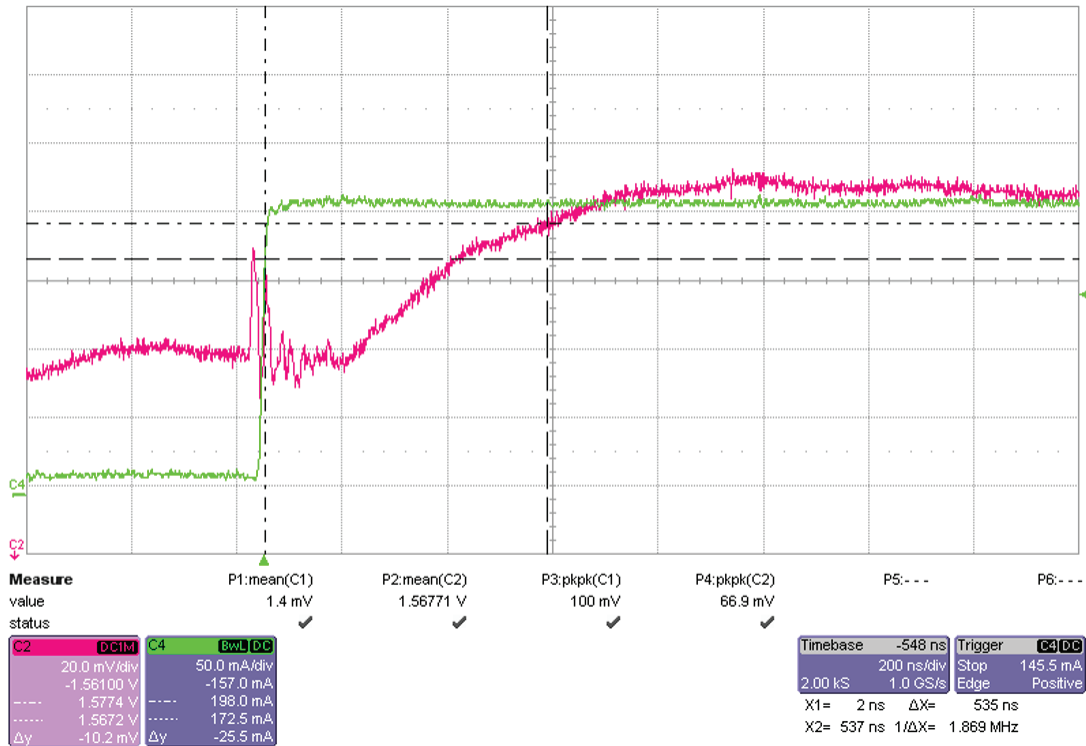
Frequency and Step Response

The ACS70331 has a bandwidth of approximately 1 MHz. However, there are a number of poles in the signal path of the

ACS70331, leading to 115 degrees of phase shift at the -3 dB frequency. The measured frequency response with a 500 mA sine wave input is shown below.



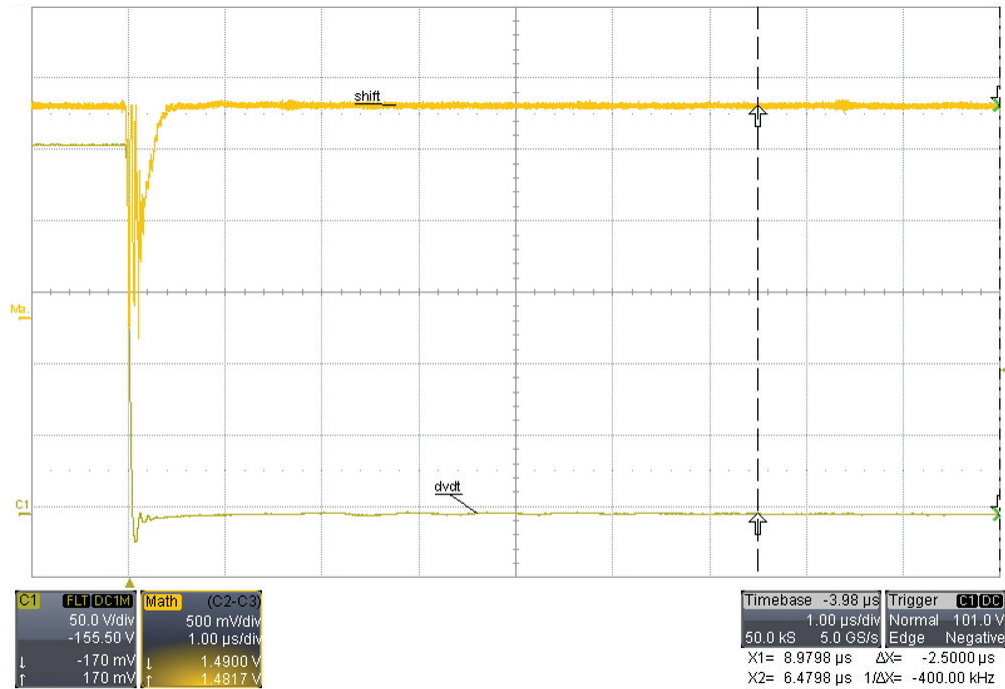
The typical step response is shown in the scope capture below.



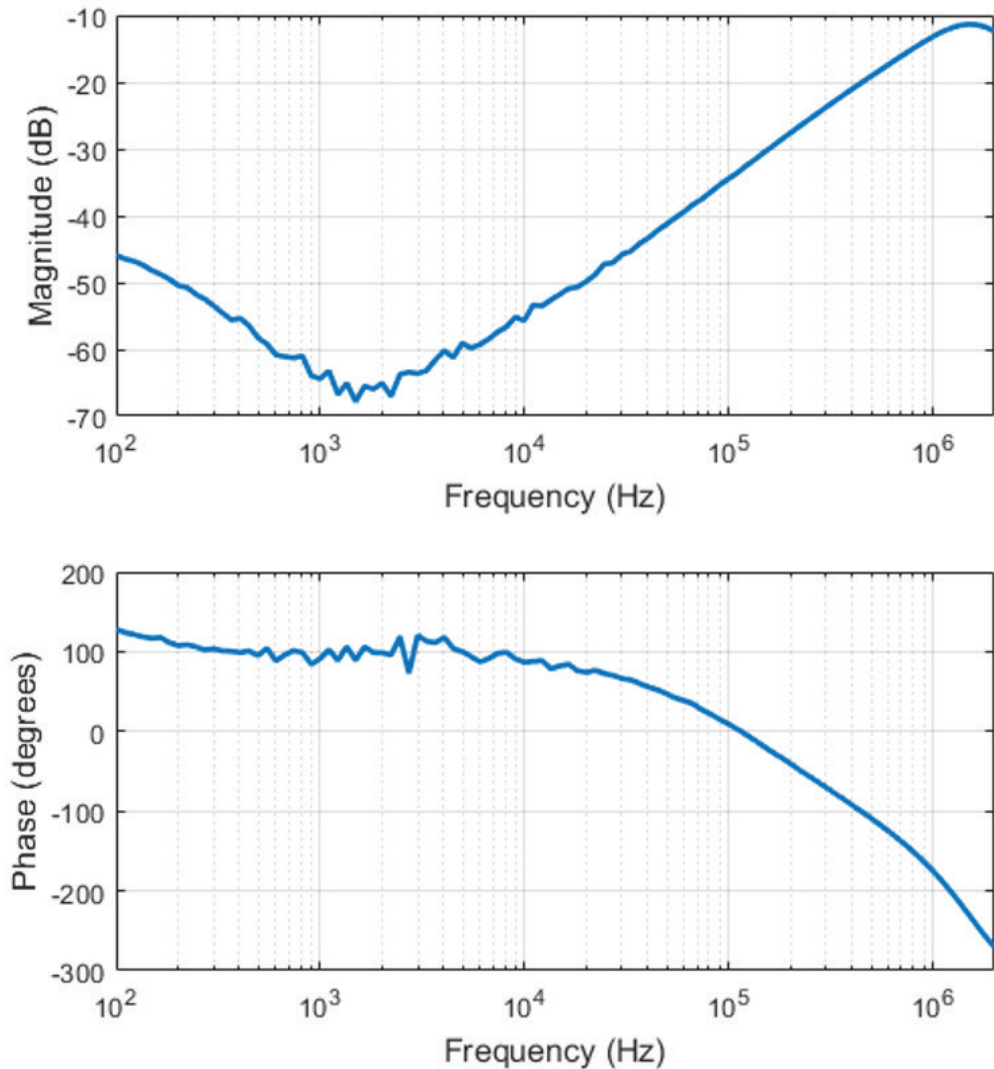
Isolation and Transient Voltage Performance

The ACS70331 uses a non-conductive die attach to isolate it from the primary conductor. This does not provide any level of safety isolation, as it only passes a hi-pot test of around 500 Vrms. It is recommended to keep the voltage from the primary to the signal leads below 100 V during operation.

The construction of the ACS70331 results in there being a capacitance from the primary conductor to the substrate of the die. When the voltage on the primary conductor changes rapidly, this can lead to a perturbation on the output of the sensor. The scope capture below shows the response of the ACS70331 to a fast transient voltage on the primary conductor. While the sensor does get disturbed significantly, it recovers within 0.5 μ s due to the high bandwidth of the sensor.



Power Supply Rejection Ratio



THERMAL PERFORMANCE AND OVERCURRENT CAPABILITY

The ACS70331 has a small primary conductor resistance of 1.1 mΩ, resulting in low power dissipation and consequently low temperature rise due to current flow through the sensor. Figure 6 shows the steady-state die temperature rise versus current of the ACS70331 on the Allegro demo board (ASEK70331), which has two layers of 1-oz. copper. At 5 A, the die temperature only rises 3.5°C. At 10 A, the die temperature increases by around 15°C, meaning that at the maximum ambient temperature of 85°C with the maximum rated continuous current of 10 A flowing, the die would just reach its maximum rated junction temperature of 100°C.

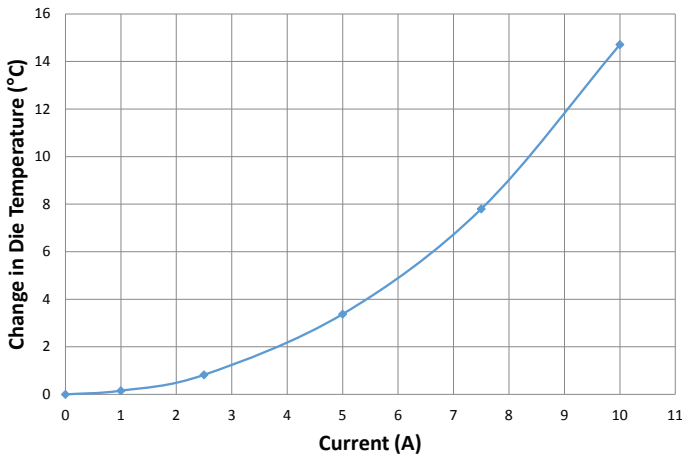


Figure 6: Change in die temperature versus current of the ACS70331 on the ASEK70331 demo board (1-oz. copper) with 22 gauge connectors to the power supply

The ACS70331 can also survive higher levels of current that only last for a short time. Figure 7 shows a curve of the time to fuse (primary loop fuses open) versus current, which one needs to operate below.

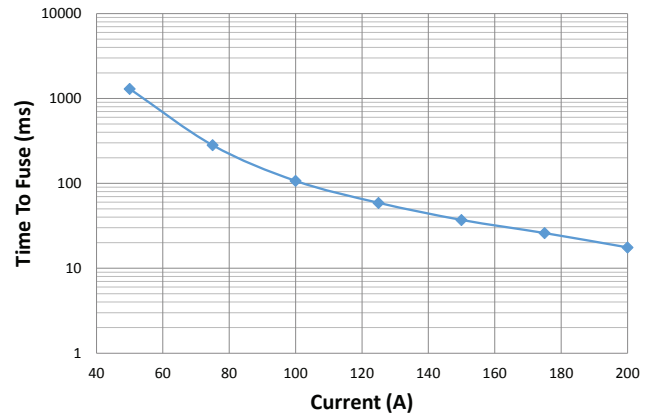


Figure 7: Time to fuse versus current of the ACS70331 on the ASEK70331 demo board (1-oz. copper) and 22 gauge connectors to the power supply

LIFETIME DRIFT

GMR elements are made up of thin layers of magnetic material, and as such, high temperature and magnetic fields can cause small shifts in the magnetization of those layers, resulting in drift in the sensor performance. The GMR elements in the ACS70331 are made up of magnetic materials which are relatively immune to the temperatures and fields seen in most commercial applica-

tions. However, extended times near the maximum rated junction temperature with applied current or field can cause the gain and offset of the sensor to shift. These shifts are dependent on the application temperature, current, and stray field, and typical drift under various application cases are given in the table below, as well as a description of the physics behind each drift.

| Test Condition | | | Typical Drift (Average + 3 sigma) | |
|----------------------|------------|-------------------|-----------------------------------|-------------|
| Junction Temperature | Current | Common Mode Field | Offset | Sensitivity |
| 125°C (408 hours) | 0 A | 0 G | ±140 mA | ±0.9% |
| 100°C (408 hours) | 1 A (DC) | 0 G | ±170 mA | ±2.3% |
| 100°C (408 hours) | 2.5 A (DC) | 0 G | ±210 mA | ±1.5% |
| 100°C (500 hours) | 5 A (DC) | 0 G | ±540 mA | ±2.8% |
| 100°C (408 hours) | 5 A (AC) | 0 G | ±150 mA | ±1% |
| 125°C (48 hours) | 0 A | 50 G | ±150 mA | ±1% |

CASE 1: CONTINUOUS CURRENT AT HIGH TEMPERATURE

In general, this is the worst case configuration for drift. High temperature and constant field will slightly rotate some of the GMR layers. Here, the field seen by two of the GMR elements in the bridge is in one direction, and the field seen by the other two GMR elements in the bridge is in the other direction. This results in two of the elements drifting in one direction and two of them drifting in the other direction, which causes an offset shift on the output of the sensor. Typically, at a given temperature and current there is a maximum amount of shift, and the time constant for the shift is around 24 hours. If one reverses the current, the shift will be in the opposite direction. Essentially, at a given temperature and current level, there is a hysteresis curve for the shift. The higher the temperature and current, the wider the hysteresis curve.

CASE 2: AC CURRENT AT HIGH TEMPERATURE

As noted in Case 1, the time constant for the offset shift in the sensor is around 24 hours, and the shift direction switches with the current direction. Because of this, AC current tends to cause little to no shift in the sensor, as the average torque on the magnetic layers is zero. This is evident in the plot below, which shows the drift when applying high DC and AC currents at 100°C.

CASE 3: STRAY FIELD AT HIGH TEMPERATURE

When stray field is applied to the sensor at high temperature, all four resistors in the bridge shift in the same direction, theoretically cancelling any drift on the output. However, due to mismatch in the elements, there is still some drift, but it is significantly less than what is seen in Case 1 or even Case 2.

DEFINITIONS OF ACCURACY CHARACTERISTICS

Hysteresis (I_H). The change in the sensor IC zero current output voltage after being subjected to a large current for a short duration. Hysteresis is due to slight magnetization of some of the ferromagnetic layers in GMR. Pulses of current in opposite directions will result in hysteresis in opposite directions. The GMR stack in the ACS70331 is optimized to have low hysteresis in comparison with more traditional stacks.

Common Mode Field Sensitivity Error Ratio ($CMFR_{SENS}$). The ratio of the shift in sensitivity due to an external stray field on the sensor relative to the field strength (%/G). This is measured in the worst case stray field configuration.

Common Mode Field Offset Voltage Ratio ($CMFR_{OFF}$). The ratio of the shift in the offset voltage due to stray field on the sensor relative to the field strength (mV/G). This is measured in the worst case stray field configuration.

Power Supply Rejection Ratio (PSRR). The ratio of the shift in V_{IOUT} due to supply voltage variation, expressed in dB. The PSRR is a small signal parameter, measured with 100 mV pk-pk over frequency.

$$PSRR = 20 \log_{10} \frac{\Delta V_{IOUT}}{\Delta V_{CC}}$$

Power Supply Offset Error ($V_{OE(PS)}$). The large signal PSRR, expressed in absolute millivolts. The power supply offset error is the variation of the offset voltage over the full supply range of the ACS70331.

Power Supply Sensitivity Error ($E_{SENS(PS)}$). The variation in sensitivity over the full supply range of the ACS70331.

Nonlinearity (E_{LIN}). The nonlinearity is a measure of how linear the output of the sensor IC is over the full current measurement range. The nonlinearity is calculated as:

$$E_{LIN} = \left\{ 1 - \left[\frac{V_{IOUT}(I_{PR(max)}) - V_{IOUT(Q)}}{2 \times V_{IOUT}(I_{PR(max/2)}) - V_{IOUT(Q)}} \right] \right\} \times 100(\%)$$

where $V_{IOUT}(I_{PR(max)})$ is the output of the sensor IC with the maximum measurement current flowing through it and $V_{IOUT}(I_{PR(max/2)})$ is the output of the sensor IC with half of the maximum measurement current flowing through it.

Sensitivity (Sens). The change in sensor IC output in response to a 1 A change through the primary conductor. The sensitivity is the product of the magnetic circuit sensitivity (G/A) (1 G = 0.1 mT) and the linear IC amplifier gain (mV/G). The linear IC amplifier gain is programmed at the factory to optimize the sensitivity (mV/A) for the full-scale current of the device.

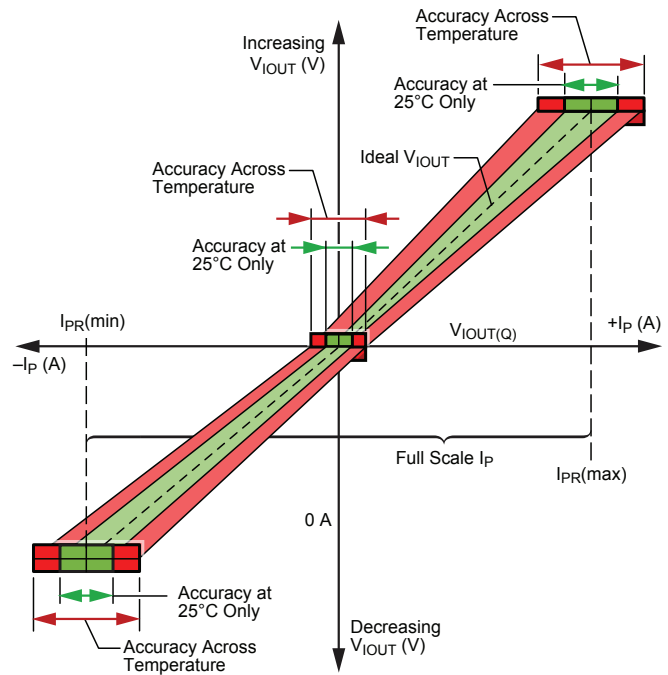


Figure 8: Output Voltage versus Sensed Current

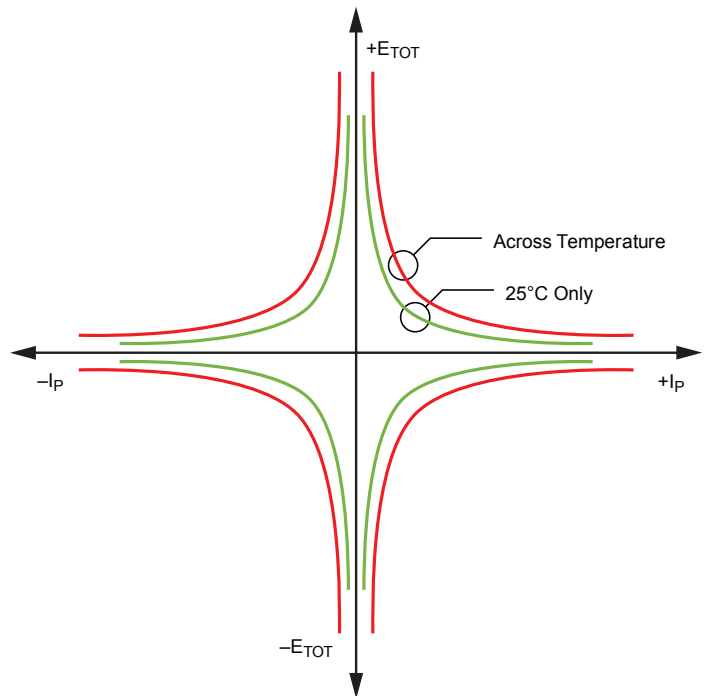


Figure 9: Total Output Error versus Sensed Current

Sensitivity Error (E_{SENS}). The variation of the sensitivity from its ideal, nominal value, Sens, expressed in percent. Sensitivity error contributes directly to the Total Output Error, percent for percent.

Zero-Current Output Voltage ($V_{\text{IOUT}(Q)}$). The output of the sensor when the primary current is zero. For a bidirectional device (measures current in both directions), it is nominally 1.5 V, and for a unidirectional device, it is nominally 0.25 V.

Offset Voltage (V_{OE}). The deviation of the device output from its ideal quiescent value of 1.5 V (bidirectional) or 0.25 V (unidirectional). To convert this voltage to amperes, divide by the device sensitivity, Sens.

Total Output Error (E_{TOT}). The difference between the current measurement from the sensor IC and the actual current (I_p), relative to the actual current. This is equivalent to the difference between the ideal output voltage and the actual output voltage, divided by the ideal sensitivity, relative to the current flowing through the primary conduction path:

$$E_{\text{TOT}}(I_p) = \frac{V_{\text{IOUT_ideal}}(I_p) - V_{\text{IOUT}}(I_p)}{\text{Sens}_{\text{ideal}}(I_p) \times I_p} \times 100 (\%)$$

The Total Output Error incorporates all sources of error and is a function of I_p . At relatively high currents, E_{TOT} will be mostly due to sensitivity error, and at relatively low currents, E_{TOT} will be mostly due to Offset Voltage (V_{OE}). In fact, at $I_p = 0$, E_{TOT} approaches infinity due to the offset. This is illustrated in Figure 8 and Figure 9. Figure 8 shows a distribution of output voltages versus I_p at 25°C and across temperature. Figure 9 shows the corresponding E_{TOT} versus I_p .

DEFINITIONS OF DYNAMIC RESPONSE CHARACTERISTICS

Power-On Time (t_{PO}). When the supply is ramped to its operating voltage, the device requires a finite time to power its internal components before responding to an input magnetic field.

Power-On Time, t_{PO} , is defined as the time it takes for the output voltage to settle within $\pm 10\%$ of its steady-state value under an applied magnetic field, after the power supply has reached its minimum specified operating voltage, $V_{CC(min)}$, as shown in the chart at right.

Fuse Power Down Time (t_{FPD}). The time interval between a) when V_{CC} goes above $V_{CC(min)}$ and b) when the sensor powers down the internal fuses.

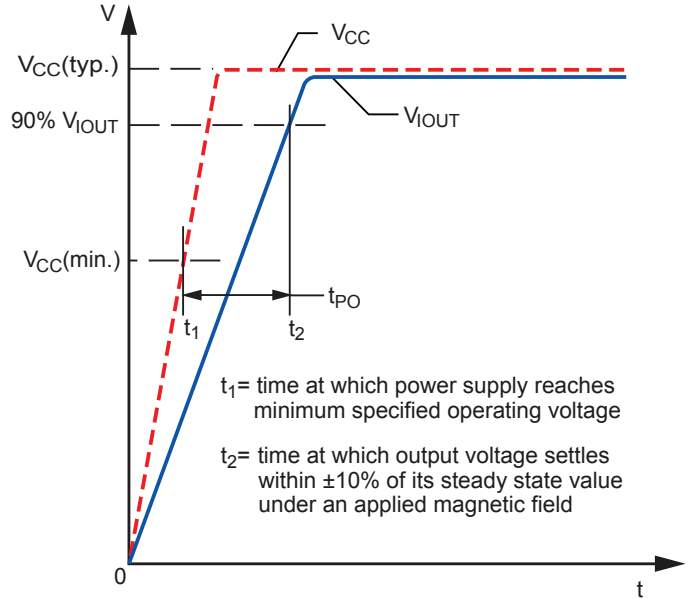


Figure 10: Power-On Time (t_{PO})

Rise Time (t_r). The time interval between a) when the sensor IC reaches 10% of its full-scale value, and b) when it reaches 90% of its full-scale value. The rise time to a step response is used to derive the bandwidth of the current sensor IC, in which $f(-3 \text{ dB}) = 0.35/t_r$. Both t_r and $t_{RESPONSE}$ are detrimentally affected by eddy-current losses observed in the conductive IC ground plane.

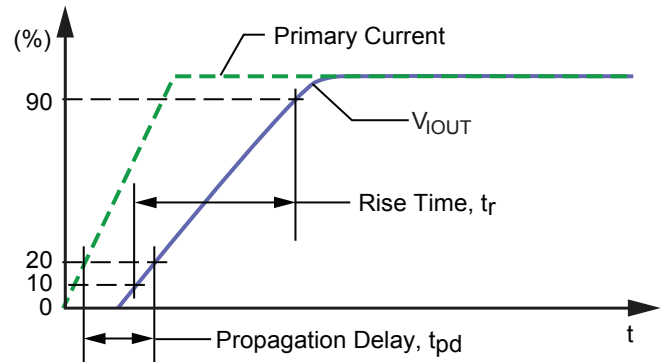


Figure 11: Rise Time (t_r) and Propagation Delay (t_{pd})

Propagation Delay (t_{pd}). The propagation delay is measured as the time interval a) when the primary current signal reaches 20% of its final value, and b) when the device reaches 20% of its output corresponding to the applied current.

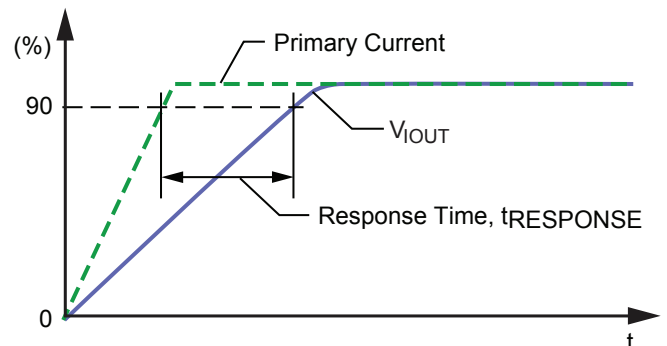


Figure 12: Response Time ($t_{RESPONSE}$)

Response Time ($t_{RESPONSE}$). The time interval between a) when the primary current signal reaches 90% of its final value, and b) when the device reaches 90% of its output corresponding to the applied current.

PACKAGE OUTLINE DRAWING

For Reference Only – Not for Tooling Use

(Reference DWG-0000222)

Dimensions in millimeters – NOT TO SCALE

Exact case and lead configuration at supplier discretion within limits shown

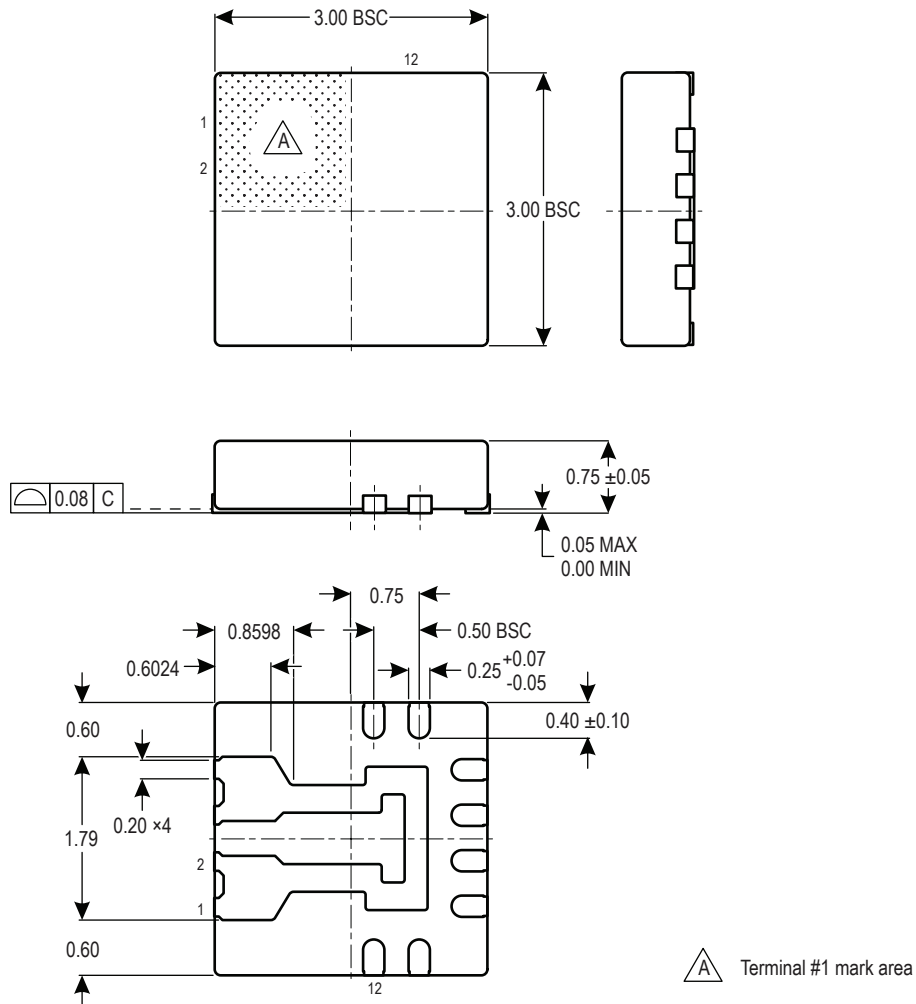


Figure 13: Package ES, 12-Contact QFN
With Fused Sensed Current Loop

Revision History

| Number | Date | Description |
|--------|------------------|-----------------|
| – | November 3, 2017 | Initial release |

Copyright ©2017, Allegro MicroSystems, LLC

Allegro MicroSystems, LLC reserves the right to make, from time to time, such departures from the detail specifications as may be required to permit improvements in the performance, reliability, or manufacturability of its products. Before placing an order, the user is cautioned to verify that the information being relied upon is current.

Allegro's products are not to be used in any devices or systems, including but not limited to life support devices or systems, in which a failure of Allegro's product can reasonably be expected to cause bodily harm.

The information included herein is believed to be accurate and reliable. However, Allegro MicroSystems, LLC assumes no responsibility for its use; nor for any infringement of patents or other rights of third parties which may result from its use.

For the latest version of this document, visit our website:

www.allegromicro.com

